HHS Public Access

Author manuscript

Alcohol. Author manuscript; available in PMC 2016 November 01.

Published in final edited form as:

Alcohol. 2015 November ; 49(7): 675–689. doi:10.1016/j.alcohol.2015.08.007.

Computed tomography assessment of peripubertal craniofacial morphology in a sheep model of binge alcohol drinking in the first trimester

Sharla M. Birch[a], **Mark W. Lenox**[b], **Joe N. Kornegay**[a,b,c], **Li Shen**[d,e], **Huisi Ai**[d], **Xiaowei Ren**[d,f], **Charles R. Goodlett**[e,g], **Tim A. Cudd**[h,+], and **Shannon E. Washburn**[h,*]

Sharla M. Birch: sbirch@cvm.tamu.edu; Mark W. Lenox: markwlenox@tamu.edu; Joe N. Kornegay: jkornegay@cvm.tamu.edu; Li Shen: shenli@iu.edu; Huisi Ai: aih@iupui.edu; Xiaowei Ren: renxi@imail.iu.edu; Charles R. Goodlett: goodlett@iupui.edu

[a]Department of Veterinary Pathobiology, Texas A&M University College of Veterinary Medicine & Biomedical Sciences, College Station, TX 77843, USA

[b]Texas A&M Institute for Preclinical Studies (TIPS), Texas A&M University College of Veterinary Medicine & Biomedical Sciences, College Station, TX 77843, USA

[c]Department of Veterinary Integrative Biosciences, Texas A&M University College of Veterinary Medicine & Biomedical Sciences, College Station, TX 77843, USA

[d]Department of Radiology and Imaging Sciences, IU School of Medicine, Indianapolis, IN 46202, USA

[e]Stark Neurosciences Research Institute, IU School of Medicine, Indianapolis, IN 46202, USA

[f]Department of Biostatistics, IU School of Medicine, Indianapolis, IN 46202, USA

[g]Department of Psychology, Indiana University Purdue University Indianapolis (IUPUI), Indianapolis, IN 46202, USA

[h]Department of Physiology and Pharmacology, Texas A&M University College of Veterinary Medicine & Biomedical Sciences, College Station, TX 77843, USA

Abstract

Identification of facial dysmorphology is essential for the diagnosis of fetal alcohol syndrome (FAS); however, most children with fetal alcohol spectrum disorders (FASD) do not meet the dysmorphology criterion. Additional objective indicators are needed to help identify the broader spectrum of children affected by prenatal alcohol exposure. Computed tomography (CT) was used in a sheep model of prenatal binge alcohol exposure to test the hypothesis that quantitative measures of craniofacial bone volumes and linear distances could identify alcohol-exposed lambs.

[*]Corresponding author: Shannon E. Washburn, Department of Veterinary Physiology and Pharmacology and Michael E. DeBakey Institute, College of Veterinary Medicine and Biomedical Sciences, 4466 Texas A&M University, College Station, TX 77843-4466, USA, Telephone: +1 979 845 1993, Fax: + 1 979 845 6544, swashburn@cvm.tamu.edu.

[+]Deceased

Pregnant sheep were randomly assigned to four groups: heavy binge alcohol, 2.5 g/kg/day (HBA); binge alcohol, 1.75 g/kg/day (BA); saline control (SC); and normal control (NC). Intravenous alcohol (BA; HBA) or saline (SC) infusions were given three consecutive days per week from gestation day 4–41, and a CT scan was performed on postnatal day 182. The volumes of eight skull bones, cranial circumference, and 19 linear measures of the face and skull were compared among treatment groups. Lambs from both alcohol groups showed significant reduction in seven of the eight skull bones and total skull bone volume, as well as cranial circumference. Alcohol exposure also decreased four of the 19 craniofacial measures. Discriminant analysis showed that alcohol-exposed and control lambs could be classified with high accuracy based on total skull bone volume, frontal, parietal, or mandibular bone volumes, cranial circumference, or interorbital distance. Total skull volume was significantly more sensitive than cranial circumference in identifying the alcohol-exposed lambs when alcohol-exposed lambs were classified using the typical FAS diagnostic cutoff of ≤10th percentile. This first demonstration of the usefulness of CT-derived craniofacial measures in a sheep model of FASD following binge-like alcohol exposure during the first trimester suggests that volumetric measurement of cranial bones may be a novel biomarker for binge alcohol exposure during the first trimester to help identify non-dysmorphic children with FASD.

Keywords

Facial dysmorphology; Prenatal alcohol; FASD; Diagnosis; Computed tomography; Anthropometry

Introduction

The teratogenic effects of alcohol abuse during pregnancy were formally identified as fetal alcohol syndrome (FAS) about four decades ago (Jones & Smith, 1973). FAS is diagnosed primarily based on three criteria: 1) presence of at least two of three characteristic dysmorphic facial features (smooth philtrum, thin upper lip, and short palpebral fissures); 2) growth deficits in height and/or weight; and 3) structural, neurologic, or functional central nervous system (CNS) abnormalities (Bertrand, Floyd, & Weber, 2005; Wattendorf & Muenke, 2005). It is now recognized that the large majority of children with untoward effects from prenatal alcohol exposure do not fully meet the criteria for a diagnosis of FAS, but still express a broad range of skeletal, neurological, developmental, behavioral, or learning abnormalities (Aase, Jones, & Clarren, 1995; Astley & Clarren, 2000; Sokol & Clarren, 1989). In 2004, the designation fetal alcohol spectrum disorders (FASD) was adopted as an umbrella term to encompass the full range of effects resulting from prenatal exposure to alcohol, with FAS being the most severe (Riley & McGee, 2005).

In the United States, FASD is the leading cause of preventable birth defects and developmental disorders (NIAAA, 2012), with a prevalence ranging from 1% of all births (Hoyme et al., 2005; Leibson, Neuman, Chudley, & Koren, 2014) to as high as 2–5% (May et al., 2009). FASD places a large burden on the economy, with estimates of the cost as high as $4 billion annually due to health care, lost productivity, and special education (Hoyme et al., 2005; Lupton, Burd, & Harwood, 2004). Despite extensive efforts to inform the public

about the risks of alcohol use during pregnancy, 7% of approximately half a million pregnant women surveyed had consumed alcohol in the previous 30 days and 1.4% reported binge drinking (CDC, 2012). Over a span of nearly 20 years, binge drinking among pregnant women has not significantly declined (CDC, 2009).

Optimal management of children with FASD depends on accurate identification of the full spectrum of children adversely affected by prenatal alcohol exposure. Diagnosis of FAS through clinical screening relies on trained recognition or anthropometric measurements of dysmorphic features of soft tissue structures of the face, yet children with FAS constitute fewer than 10% of all children with FASD. Reliable indicators of adverse effects of prenatal alcohol exposure are needed to help identify the much larger number of children with FASD who do not meet the facial dysmorphology criterion. Quantitative analysis of craniofacial bones, which are derived from embryonic neural crest cells that are sensitive to alcohol exposure during neurulation (Smith, Garic, Flentke, & Berres, 2014), provides a potential approach for identifying a more sensitive indicator. Relatively little work has been done to evaluate the underlying craniofacial bones, and its potential use as a quantitative indicator to identify children with FASD is largely untapped.

Binge drinking during the first trimester (including prior to pregnancy recognition) is the most common pattern of risk drinking in women of childbearing age (Conover & Jones, 2012; Maier & West, 2001; Ramadoss, Hogan, Given, West, & Cudd, 2006). Craniofacial bone changes are an appropriate candidate as a structural biomarker for binge drinking, in part because of the spatiotemporal links between embryonic CNS and craniofacial development during the first trimester. Bones that form the neurocranium (frontal, parietal, and occipital bones) are derived principally from the neural crest and paraxial mesoderm, whereas bones that form the viscerocranium (mandible, maxilla, nasal, lacrimal, and jugal bones) originate primarily from the first two pharyngeal arches (Moore, 2013). During neurulation, neural crest cells originate at the junction of the neural folds and eventually the cells migrate to various locations throughout the embryo to form body structures (Smith et al., 2014). A subset of neural crest cells, cranial neural crest cells, forms structures of the face (bones, cartilage, and cranial nerves) (Sulik, Cook, & Webster, 1988), and are highly sensitive to alcohol. Damage to these cells results in dysmorphic craniofacial features and some associated brain abnormalities associated with FAS (Cartwright & Smith, 1995; Rovasio & Battiato, 1995; Smith, 1997).

In humans, key events over the first trimester of pregnancy (O'Rahilly & Müller, 1996) include neurulation (spanning postfertilization days 22–31), which involves formation of the neural tube and neural crest, with anterior neuropore closure by day 30. Emergence of the full five-vesicle stage is evident at 5 weeks, along with formation of the pontine flexure, optic cup, and nasal pit. Formation of the telencephalic cortical plate begins at 7–8 weeks with the appearance of the five zones of the emerging cerebral cortex (marginal, cortical plate, subplate, subventricular, and ventricular zones). By comparing the timing of the same events during embryonic development in sheep (that have a 147-day gestation), it is possible to establish temporal equivalence in sheep to the first 8 weeks of human development. In sheep, neural tube formation extends into the 3rd gestational week and the anterior neuropore closes by gestational day (GD) 21. The five-vesicle stage is evident in the 4th

gestational week, while the cortical plate begins forming in the lateral wall of the telencephalon at GD35. By GD40, the lateral wall has formed a defined cortical plate and the five zones of the emerging cerebral cortex are evident (Reynolds & Møllgård, 1985). Comparatively, the first 40 days of embryonic development in the sheep are roughly equivalent to the first 8 weeks of human development.

Experimental animal models, primarily mouse models, have shown that binge-like alcohol exposure during the first trimester equivalent is sufficient to induce abnormal craniofacial development. These studies have identified key roles of dose and timing of prenatal alcohol exposure in producing craniofacial effects that model some of those seen in FAS (Sulik, 1984; Sulik et al., 1988). Specifically, they have shown quantitatively that measurable craniofacial changes do occur (Anthony et al., 2010; Hernandez-Guerrero, Ledesma-Montes, & Loyola-Rodriguez, 1998; Lipinski et al., 2012; Robin & Zackai, 1994). A major goal of the current study was to extend this approach to a well-defined sheep model of binge alcohol exposure during a portion of the first trimester equivalent, to assess whether quantitative analyses of craniofacial bone volumes using computed tomography (CT) in 6-month-old (peripubertal) lambs could accurately predict exposure.

In this study, sheep were evaluated at 6 months of age because we wanted a target age comparable to middle school-aged children about to enter puberty during early adolescence. Sheep reach puberty when they attain 50–70% of their mature body weight, typically between 7–8 months of age, depending on breed (*The Merck Veterinary Manual*, 2005). Therefore, the developmental status of these lambs may be analogous to children in their middle-school years with undiagnosed FASD that have developmental, behavioral, and/or learning deficits often identified by educators. Additionally, we sought to compare the relative accuracy of classifications of prenatal alcohol exposure through a single CT scan, which allowed measurement of both cranial bone volumes and linear distance measures taken from bone (cranial) and soft tissue (facial) landmarks, along with cranial circumference. If confirmed, these quantitative approaches in this sheep model could provide new indices of the effects of prenatal alcohol exposure that may prove more sensitive than traditional FAS diagnostic indices (head circumference; facial morphometrics). This could translate into improved identification of children with FASD.

Measures evaluated in the current study include the volume of the bones of the neurocranium and viscerocranium, along with linear measurements of the skull, face, and cranial circumference. CT was utilized because it is non-invasive, readily available in most hospitals, produces high-resolution, three-dimensional images, and one scan allows measurement of bony and soft tissue structures of the face. CT has been effectively used to study fixation artifacts in embryologic studies (Schmidt et al., 2010) and recently in studies of craniofacial dysmorphology in mouse models of FASD (Kaminen-Ahola et al., 2010; Shen et al., 2013). Repeated weekend binge drinking (3 consecutive days per week) over the first 8 weeks of human pregnancy was modeled from GD4-41 in the sheep with two binge-like alcohol treatments. The first treatment modeled heavy binge drinking (2.5 g/kg per day, peak blood alcohol concentrations [BACs] above 250 mg/dL) and the second treatment modeled more typical binge drinking (1.75 g/kg per day, peak BACs around 200 mg/dL). We hypothesized that, relative to the control groups, lambs given binge-like prenatal alcohol

exposure would: 1) have reduced CT-derived volumes of the skull bones; 2) have reduced cranial circumferences; 3) have altered craniofacial morphometrics of bone as well as face; and 4) be classified accurately in terms of prenatal alcohol exposure based on one or more of these measures. Because FAS is often associated with binge drinking during the first trimester, comparisons between the two binge treatment conditions could help determine whether more intense binge exposure episodes produce increasingly severe effects on craniofacial morphometrics or skull bone volumes.

Materials and methods

Animals

All animals and experimental procedures were approved by the Institutional Animal Care and Use Committee (IACUC) at Texas A&M University. Prior to breeding, Suffolk ewes (aged 2–5 years) received multi-species Clostridium bacterin-toxoid (Covexin 8, Intervet/ScheringPlough Animal Health, Summit, NJ) 2 mL intramuscularly, albendazole (Valbazen Suspension 7.5 mg/kg, Pfizer Animal Health, New York, NY) 0.75 mL/25 lb. of body weight orally, and ivermectin (Ivomec Drench for Sheep 0.8%, Merial, Duluth, GA) 3 mL/26 lb. body weight orally. The day of mating (the day that the ewes were marked by the ram) was designated as GD 0, and ewes entered the experiment the next day. Ewes were penned individually for the experiment but had visual contact at all times with herd mates in adjacent pens in an environmentally regulated facility (22°C and a 12:12-h light/dark cycle). Ewes entering the experiment were randomly assigned to one of four treatment groups: normal control (NC), saline control (SC), binge alcohol (BA), or heavy binge alcohol (HBA). Pregnancy was confirmed ultrasonographically on GD25, and if ewes were not pregnant, they were removed from the experiment. Ewes were fed a “complete” ration (TAMU Ewe Ration, Nutrena, Cargill, Minneapolis, MN) designed to meet 100% NRC requirements as calculated by ARIES (software version 2007, University of California, Davis) and had free access to drinking water. Maternal food consumption was monitored daily. All subjects consumed all feed offered.

Just before parturition, ewes were moved to a covered pen outside where they lambed naturally. At birth, newborn lambs were weighed and measured, and their navels were dipped in iodine (VetOne Stronger Iodine, 7%, MWI, Meridian, ID). They were also given oxytetracycline (Liquamycin®, LA-200®, 200 mg/mL, Pfizer Animal Health, New York, NY) 1 mL intramuscularly and selenium/vitamin E (BO-SE®, 1 mg/mL, Intervet/Schering-Plough Animal Health, Summit, NJ) 0.5 mL subcutaneously. Each ewe was checked for satisfactory milk production, and lambs were closely monitored for nursing, weight gain, and health status over the next 2 months. At 1 and 2 months of age, lambs were vaccinated using multi-species clostridium bacterin-toxoid (Covexin 8, Intervet/Schering-Plough Animal Health, Summit, NJ) 2 mL intramuscularly. Nursing lambs and ewes remained together until the lambs reached 2 months of age, at which time they were separated from their mothers and weaned. Ewes were removed from the premises, and weaned lambs remained in the same outdoor covered pens for the rest of the study. At weaning, lambs received moxidectin (Cydectin® Oral Drench for Sheep 0.1%, 1 mg/mL, Boehringer Ingelheim, St. Joseph, MO) 0.2 mL/kg body weight orally, amprolium (Corid® 9.6% Oral

Solution, Merial, Duluth, GA) 0.5 mL/kg orally once daily for 10 days, and vitamin B1 (Thiamine Hydrochloride, 500 mg/mL, Rafter 8 Products, Calgary, Alberta, Canada) 1.5 mL subcutaneously once daily every third day for a total of four treatments. Weaned lambs were fed a "complete" ration (Ringmaster Start-To-Finish Show Lamb Pellets, Nutrena, Minneapolis, MN) designed to meet 100% NRC requirements as calculated by ARIES (software version 2007, University of California, Davis) and had free access to drinking water. At 6 months of age, lambs were euthanized using sodium pentobarbital (Beuthanasia®, Intervet/Schering-Plough Animal Health, Summit, NJ) 75 mg/kg intravenously. Computed tomography (CT) imaging was performed immediately after euthanasia.

Treatment groups

Ewes (n = 36) were randomly assigned to one of four treatments – normal control (NC) group (n = 8 ewes), the saline control (SC) group (n = 8 ewes), the binge alcohol (BA; 1.75 g/kg) group (n = 8 ewes), and the heavy binge alcohol (HBA; 2.5 g/kg) group (n = 12 ewes). An intravenous catheter (16-gauge, 5.25-inch Angiocath™; Becton Dickinson, Sandy, UT) was placed into the jugular vein of each ewe (except for the NC group) on GD 4. Beginning on this day, alcohol (2.5 or 1.75 g/kg body weight) or saline was administered intravenously over a 1-h period via a pump (VetFlo® 7701B IV Vet Infusion Pump, Grady Medical, Temecula, CA). The alcohol solution was prepared by adding 95% ethanol to sterile 0.9% saline to achieve a 40% w/v alcohol solution. Solutions were prepared under aseptic conditions and were passed through a 0.2-μm bacteriostatic filter. The saline control group received an infusion of isotonic saline (0.9%) that was equal in volume to the alcohol infusions. Infusions were administered on three consecutive days per week from GD4–41, followed by four days without treatment (18 treatments total). Lambs produced from ewes in the four treatment groups that entered the imaging study included 8 NC lambs (1 female, 7 males), 8 SC lambs (4 females, 4 males), 8 BA lambs (6 females, 2 males), and 12 HBA lambs (6 females, 6 males).

Maternal blood alcohol concentration

Blood was drawn from the jugular vein of each ewe 1 h after alcohol infusions began to measure peak BAC as previously described (Washburn, Sawant, Lunde, Wu, & Cudd, 2013). A 20-μL aliquot of blood was collected in a microcapillary tube and transferred into a vial containing 0.6 N perchloric acid and 4 mM n-propyl alcohol (internal standard) in distilled water. The vial was tightly capped with a septum-sealed lid and stored at room temperature until analysis by headspace gas chromatography (Varian Associates model 3900, Palo Alto, CA) at least 24 h after collection.

Computed tomography imaging

Images were acquired on a computed tomography (CT) scanner (Biograph mCT®, Siemens Medical, USA) that operated at 120 kVp and 300 mA maximum cube current. In the standard mode of operation, the distance from the detector to the source was 1.0856e+003 mm and source to subject distance was 595 mm. The data collection diameter of the scan field of view (SFOV) was 500 mm, and the reconstruction diameter of the display field of view (DFOV) was 300 mm. The matrix was 512 × 512, pixel size was 0.59 mm, slice

thickness was 1 mm, and voxel volume was 0.348 mm^3. The image acquisition was performed on animals immediately after euthanasia. Before animal scanning, daily system calibration was performed for accuracy. Long-term scanner maintenance was performed in compliance with the operating manual (Siemens Biograph mCT® versions VG10A, VG21A, VG30A, VG40A, chapters 7 and 12).

Image analysis

Amira Software (Visage Imaging, Inc., San Diego, CA) was used for bone segmentation and acquisition of skull measurements and craniofacial measurements. After three-dimensional (3D) reconstruction of the head scan, bony tissues were segmented (identified) as previously described (Shen et al., 2013). A threshold of 160 HU (Hounsfield Units) was used to complete all bony tissue segmentations and skull measurements, and −350 HU was used for soft tissue facial measurements. Amira Software was used to visualize soft tissue structures and underlying craniofacial bones and then manually extracted a total of 29 measurements: 1) nine 2D skull craniofacial measurements (distance, mm): upper facial depth, lower facial depth, orbital height and width, minimal frontal width, bitragal width, bigonial width, interorbital distance, and nasal length (see Table 1 and Fig. 1); 2) ten 2D craniofacial soft-tissue measurements (distance, mm): nasal width, nasal length, nasal bridge length, philtrum length, lower facial height, mid-facial depth, lower facial depth, palpebral fissure length, inner canthal width, and outer canthal width (see Table 1 and Fig. 2); 3) eight 3D individual skull bone volumes plus total skull bone volume (volume; mm^3): mandible, frontal, parietal, occipital, maxilla, nasal, lacrimal, and jugal bones (see Fig. 3), with total skull the sum of all eight; and 4) 2D cranial circumference (distance, mm). Though cranial circumference was obtained as part of the skull distance measures in the lambs, it was separated from the craniofacial measures for the purposes of initial analyses. This was done because head circumference is typically obtained separately from the dysmorphology exam in clinical settings as part of the diagnostic measures to identify children with FAS, and it is interpreted separately from facial dysmorphology (Jones et al., 2009). All measurements were taken by one of the authors (SMB) who was blinded to the treatment groups. To decrease measurement error, each measurement was repeated in triplicate with subsequent measures taken only if the first three measurements differed by >2mm. In instances in which >3 measurements were taken, outliers >2mm were not used. The nineteen 2D craniofacial measurements and the cranial circumference measurement were acquired utilizing a measurement tool in Amira. The eight bones of the skull were manually segmented, and their volumes were calculated based on the segmentation results. For the bilateral linear measurements of the face and skull, preliminary analyses indicated there were no significant differences between the left and right sides, so only the left side of all bilateral measurements of the face and skull were used for subsequent analyses. Total skull bone volume was calculated by adding all of the individual bone segmentations together (left and right sides where applicable). Ear measurements were not taken because the ears were inadvertently cropped in the CT output file.

Statistical analysis

Given the unequal numbers of males and females in the NC and BA groups and the low number of lambs of each sex across treatment groups overall, the power to detect potential

sex differences was very limited. The data were first screened for potential differences between males and females. This was to determine whether the male and female data could be combined within groups for the purposes of statistical analysis without confounding the analysis of prenatal treatment. The NC group had only one female and the BA group had only two males. The within-group ranking of the data of those subjects was determined and each fell within the range of the majority sex of the group. Therefore, the individual data did not skew the within-group distribution for any measure for either the NC or BA groups. For the two groups with equal numbers of males and females (SC and HBA), a two-way analyses of variance (ANOVA) with sex and treatment as grouping factors was calculated. None of the measures showed a significant main or interactive effect of sex, so the data of males and females were combined within groups for subsequent analyses of variance.

Treatment effects on measurements of skull bone volumes, skull distances, face distances, and cranial circumference were first analyzed with one-way between-subjects ANOVA using Bonferroni-corrected alpha levels to set the significance level within each set of data. Thus, for the nine skull bone volumes and nine skull distance measures, a Bonferroni-corrected alpha level of 0.0056 (= 0.05/9) was used for the nine univariate ANOVAs. For the ten face distance measures, the Bonferroni-corrected alpha level was 0.005 (= 0.05/10). For cranial circumference, the alpha level was 0.05. Measures that met the Bonferroni-corrected alpha level on the univariate test were then analyzed using pairwise comparisons among the four treatments within each measure, and the multiple comparisons were corrected by the Holm-Sidak method ($p < 0.05$). In addition, two different one-way between-subjects analyses of covariance (ANCOVA) were calculated for individual skull bone volumes. The first included covaried total skull bone volume and sex, while the second were covaried cranial circumference and sex. Separate ANCOVAs were also calculated for the facial and skull bone linear distances, covarying for cranial circumference and sex. The main purpose of these covariance analyses was to determine the extent to which individual skull bone volumes (or craniofacial linear measures) could provide quantitative evidence of the effects of binge alcohol treatment beyond that which might be associated with reduced head size, as well as to control for any influences of sex differences. This approach follows a publication that assessed similar measures in a prenatal mouse model (Shen et al., 2013). To determine whether total bone volume provides a better identification of alcohol-exposed lambs than cranial circumference (akin to head circumference in FAS screening), the 10th percentile was calculated for each measure. Each distribution, total skull bone volume, and cranial circumference, from the NC and SC groups (not significantly different) was combined to form control distributions for each measure. Lambs in the BA and HBA groups were then classified based on whether or not they were <10th percentile of the control distribution for each measure (similar to the FAS screening cutoff). The relative sensitivity of the two measures was determined by comparing the number of lambs in the 10th percentile of the two measures using Fisher's Exact Test.

Discriminant analysis

Univariate discriminant analyses of the craniofacial bone measures were examined for six pairwise comparisons: NC vs. HBA, NC vs. BA, NC vs. SC, SC vs. BA, SC vs. HBA, and BA vs. HBA. Univariate Receiver Operating Characteristic (ROC) analysis was

implemented using Matlab (The MathWorks, Inc., Natick, MA) and was performed on each of the following measures: 1) nine skull volume measures, 2) nine skull distance measures, and 3) ten face distance measures; cranial circumference was included in each of the three data sets. Area under the ROC curve (AUC) was reported. The best overall classification accuracy for percent of all animals correctly classified on the ROC curve, its corresponding sensitivity for percent of cases correctly classified, and its corresponding specificity for percent of controls correctly classified, were also reported in each comparison.

Results

Maternal blood alcohol concentration

The mean ± SEM maternal BACs at the end of alcohol infusion (1 h; point in time at which BACs are known to peak) were significantly higher in the HBA treatment (280.0 ± 9.7 mg/dL) compared to the BA treatment (198.9 ± 8.6 mg/dL) ($p = 0.001$).

Fetal and 6-month-old body weights

There were no significant differences between groups with regard to fetal birth weight (NC, 5.71 ± 0.35 kg; SC, 5.74 ± 0.33 kg; BA, 5.13 ± 0.49 kg; HBA, 4.68 ± 0.31 kg) and 6-month-old body weight (NC, 36.59 ± 4.33 kg; SC, 38.72 ± 4.04 kg; BA, 34.09 ± 2.25 kg; HBA, 33.02 ± 1.71 kg).

Correlations among measures

As expected, Pearson correlations among all nine skull volume measures and the cranial circumference were strongly positive (see Table 2), and all were statistically significant ($p < 0.001$). The correlation coefficients ranged from $r = 0.640$, between the nasal and parietal bones, to $r = 0.955$ between total skull bone volume and frontal bone. Each of the bone volumes were highly correlated with cranial circumference ($r = 0.716$ to 0.939).

Pearson correlations among the nine skull distance measurements and cranial circumference were all positive (see Table 3), and 53% were statistically significant ($p < 0.001$). The significant correlations ranged from $r = 0.530$, between the interorbital distance and orbital height, to $r = 0.897$ between the bitragal width and cranial circumference. Notably, all of the skull distance measures except orbital width and skull nasal length were significantly correlated with cranial circumference ($r = 0.579$ to 0.897). Orbital width did not correlate significantly with any of the other skull measures and skull nasal length significantly correlated with only one skull measure (lower facial depth).

Pearson correlations among ten facial measurements and the cranial circumference were all positive and 43.6% were statistically significant (see Table 4). The significant correlation coefficients ($p < 0.001$) ranged from $r = 0.460$, between the outer canthal width and lower facial depth, to $r = 0.977$ between the nasal bridge length and facial nasal length. All of the facial distance measures except the lower facial height and palpebral fissure length were significantly correlated with the cranial circumference ($r = 0.543$ to 0.837). Palpebral fissure length did not correlate significantly with any of the other facial measures.

Pearson correlations between the ten facial distance measures and the nine underlying skull distance measures resulted in 29 positive correlations ($p < 0.001$) out of 90 (32%, see Table 5). A majority of these 29 reflected common structural features between facial landmarks and underlying skull structures (e.g., lower facial depth in the face correlated with the same measure in bone; inner and outer canthal widths in facial measures correlated with bone measures of minimal frontal width, bitragal width, bigonial width, and interorbital distance; facial nasal length correlated with bone lower facial depth, etc.). Mid-facial depth (akin to the "flattened mid-face" of FAS) significantly correlated with six of the nine bone distance measures. Palpebral fissure length and philtrum length are two facial measures most directly comparable to measures used in FAS dysmorphology evaluations. Palpebral fissure length was not significantly correlated with any underlying bone measure and philtrum length was significantly correlated only with orbital height.

Skull bone volumes and cranial circumference

As shown in Fig. 4, significant effects of prenatal treatment were evident in eight of the nine volumetric skull measures (Bonferroni-corrected $\alpha = 0.0056$) and in the cranial circumference measure ($p < 0.05$). Bones with significant treatment effects included the mandible ($F[3,35] = 15.988$, $p < 0.001$), frontal ($F[3,35] = 24.906$, $p < 0.001$), parietal ($F[3,35) = 26.724$, $p < 0.001$), occipital ($F[3,35] = 18.285$, $p < 0.001$), maxilla ($F[3,35] = 12.850$, $p < 0.001$), lacrimal ($F[3,35] = 16.894$, $p < 0.001$), jugal ($F[3,35] = 14.740$, $p < 0.001$), total skull bone volume ($F[3,35] = 23.944$, $p < 0.001$), and cranial circumference ($F[3,35] = 15.089$, $p < 0.001$). Pairwise group comparisons (Holm-Sidak $p < 0.05$) confirmed that the bone volumes of the HBA and BA groups were significantly reduced relative to the NC and SC groups for all skull bones except the nasal bone, the total skull bone volume, and the cranial circumference. There were no significant differences between the BA and HBA groups, or between the NC and the SC groups.

Covariance analyses using either total skull bone volume or cranial circumference and sex as covariates were used to assess alcohol treatment effects on individual skull bone volumes. This was done to determine if the individual bone volumes would remain significant after the effects of head size or total skull bone volume and sex differences were removed. After covarying for total skull bone volume and sex, treatment effects on volumetric skull measures were no longer significant (Bonferroni-corrected $\alpha = 0.00625$). This was consistent with the strong correlations between total skull bone volume and the volume of each individual bone. After covarying for cranial circumference and sex, significant effects among the four treatment groups were found in four of the nine volumetric skull measures (Bonferroni-corrected $\alpha = 0.0056$; Fig. 5). These included the frontal, parietal, and occipital bones, as well as the total skull bone volumes. Pairwise comparisons (Holm-Sidak $p < 0.05$) showed the HBA treatment differed from both NC and SC groups for the parietal and occipital bones. The occipital bone was the only bone volume measure to show a significantly greater reduction in the HBA treatment compared to the BA treatment, suggesting a dose-dependent effect. Thus, when variance associated with cranial circumference (and sex) was statistically controlled, the parietal and occipital bones still distinguished the HBA group from the NC and SC groups.

Craniofacial distance measures

Significant treatment effects were evident in five of the nine skull distance measures (Bonferroni-corrected $\alpha = 0.0056$; Fig. 6), including the upper facial depth ($F[3,35] = 8.997$, $p < 0.001$), bitragal width ($F[3,35] = 10.949$, $p < 0.001$), interorbital distance ($F[3,35] = 7.806$, $p < 0.001$), and nasal length ($F[3,35] = 5.575$, $p < 0.001$). Holm-Sidak pairwise group comparisons showed significant differences ($p < 0.05$) between the BA and HBA groups and the NC and SC groups for upper facial depth, bitragal width, and interorbital distance. No significant differences were found between the BA and HBA groups, or between the NC and SC groups in these three skull distance measures. Bigonial width showed differences between the HBA and SC groups, but HBA did not differ significantly from NC. Nasal length showed differences between the BA and HBA groups, but neither of those was significantly different from either the NC or SC groups.

For the facial distance measures, significant treatment effects were found in five of the ten measures (Bonferroni-corrected $\alpha = 0.005$; see Fig. 7), including the philtrum length ($F[3,35] = 5.244$, $p < 0.001$), mid-facial depth ($F[3,35] = 6.946$, $p < 0.001$), lower facial depth ($F[3,35] = 5.195$, $p < 0.001$), inner canthal width ($F[3,35] = 15.097$, $p < 0.001$), and outer canthal width ($F[3,35] = 6.618$, $p < 0.001$). However, follow-up Holm-Sidak pairwise group comparisons for these five measures indicated that only the inner canthal width showed significant reductions ($p < 0.05$) in both alcohol-exposed groups compared to the two control groups. None of the other measures showed significant differences between the alcohol-exposed and both control groups. Covariance analyses were performed to evaluate the effects of cranial circumference and sex on the nine skull distance measures (Bonferroni-corrected $\alpha = 0.0056$) and the ten face distance measures (Bonferroni-corrected $\alpha = 0.005$). None of the skull or face measures remained significant between the alcohol-exposed groups and the control groups.

Discriminant analyses

Area under ROC curve (AUC) results from the univariate ROC analyses are shown in Table 6A, 6B, and 6C. Several bone volumetric measures were identified as best predictors in classifying between alcohol-exposed groups and control groups across the ROC analysis of the six treatment pairs (see Table 6A). The mandible, frontal bone, parietal bone, and total skull bone volumes achieved an AUC of 0.99–1.0, with the best overall accuracy of 100% (sensitivity 100%, specificity 100%). The occipital bone provided the best discrimination between the BA and HBA groups (AUC = 0.708; accuracy of 75%, sensitivity and specificity of 75%). For the skull distance measures (see Table 6B), the interorbital distance was the best predictor in distinguishing between an alcohol and control treatment (AUC between 0.984–1.0) with overall accuracies between 93.8–100% (sensitivities between 87.5–100%, specificities of 100%). For the facial soft-tissue measures (see Table 6C), the inner canthal width was the best predictor in distinguishing between an alcohol and control treatment. The AUC ranged between 0.906–1.0, and accuracies between 90–100% (sensitivities 87.5–100%, specificities 75–100%). The cranial circumference was the next best predictor in distinguishing between an alcohol and control treatment, with AUC ranging between 0.875–0.984, and accuracies between 93.8–95% (sensitivities 87.5–100%, specificities 87.5–100%). Of the skull and facial distance measures, the best predictors to

classify between the BA and HBA groups were the skull nasal length (AUC 0.802; overall accuracy of 75%; sensitivity 58.3% and specificity 100%) and nasal bridge length (AUC 0.781; overall accuracy of 75%; sensitivity 83.3% and specificity 62.5%).

Relative sensitivity of total skull bone volume and cranial circumference

From the discriminant analysis (above and Table 6A), total skull bone volume was 100% accurate in classifying alcohol-exposed and control lambs, more accurate than the cranial circumference (with which it was highly correlated, $r = 0.939$). The effect size of the alcohol treatment for total skull bone volume (Cohen's $d = 2.81$) was larger than the effect size for cranial circumference (Cohen's $d = 2.23$). In the context of potential usefulness of total skull bone volume as a screening measure to help identify a larger proportion of individuals with FASD, the relative sensitivity of total skull bone volume (a novel candidate measure) was compared to the cranial circumference (similar to head circumference in clinical screening in which scores <10th percentile are used to help diagnose FAS). Lambs of the NC and SC groups were combined (n = 16), and the 10th percentile of this combined control group was established for both the cranial circumference measure (390.7 mm) and the total skull bone volume measure (254,358 mm^3). Alcohol-exposed lambs of both groups (BA and HBA) were then predicted based on whether or not they were less than the 10th percentile cutoff. For cranial circumference, 14 out of 20 alcohol-exposed lambs (70%) were under the cutoff (7/8 BA; 1/12 HBA), whereas all 20 of the alcohol-exposed lambs (100%) were under the cutoff for total skull volume. A two-tailed Fisher's Exact Test confirmed that the classification based on total skull bone volume was significantly more sensitive than the one based on cranial circumference ($p = 0.020$).

Discussion

Although facial dysmorphology is a cardinal feature of FAS, children with FASD may not have identifiable features or their facial features may be too subtle to detect reliably on clinical exam (Streissguth, 1994; Streissguth et al., 1991; Wattendorf & Muenke, 2005). As a result, many children exposed prenatally to alcohol are not recognized as having FASD until later in adolescence when unruly behavior or developmental and learning disabilities become problematic. This study of lambs born to ewes given alcohol during the first trimester equivalent tested whether more sensitive structural indices could be achieved from a single CT scan of the head. Quantitative measures obtained from this scan provide a novel biomarker for prenatal alcohol exposure utilizing individual bone volumes and collectively, the total skull bone volume. The scan also allows for morphometric measures, skull bone and soft tissue, which model anthropometric studies in humans (Astley, 2006; Hoyme et al., 2005; Moore et al., 2007) and rodents (Anthony et al., 2010; Shen et al., 2013).

An important discovery from this sheep model is that quantitative volume measures of the bones of the neurocranium may be one of the most sensitive structural indicators of the effects of binge alcohol during the first 8 weeks of human pregnancy. Both the binge alcohol (BA) and heavy binge alcohol (HBA) treatments resulted in significant and severe reductions in total skull bone volume, volumes of the frontal, parietal, occipital, maxilla, mandible, lacrimal, and jugal bones, as well as cranial circumference. After statistically

controlling for smaller cranial circumference in the alcohol-exposed groups, significant reductions in the volumes of the parietal and occipital bones were evident in the HBA group. Discriminant analysis showed that the frontal bone, parietal bone, and total skull bone volumes achieved 100% sensitivity and specificity in predicting prenatal treatment (alcohol or control). Volumes of these bones were better predictors of alcohol exposure than cranial circumference, and were consistent with the greater effect size of alcohol treatment for total skull bone volume ($d = 2.81$) and cranial circumference ($d = 2.23$). All alcohol-exposed lambs were at or below the 10th percentile of the control lamb distribution for total skull bone volume. The sensitivity of classification of alcohol-exposure based on this 10th percentile cutoff for total skull volume was significantly better than a similar classification based on a 10th percentile cutoff for cranial circumference. Taken together, these findings suggest that CT-derived measures of neurocranial bone volumes may provide a novel method for identifying children with FASD.

Cranial circumference in this model is directly parallel to reduced head circumference in FAS. Head circumference is routinely evaluated on a physical exam (Hoyme et al., 2005; Jones et al., 2010) and is a simple, direct, and easily obtained measure that has population norms. The smaller head circumference found in children with FAS (Carter, Jacobson, Sokol, Avison, & Jacobson, 2013; Ortega-García et al., 2012) has been modeled in mice exposed to alcohol prenatally (Shen et al., 2013) and was replicated in this study. However, the results in this study indicate that total skull volume is more sensitive and more accurate than cranial circumference in predicting prenatal alcohol exposure, even though the two measures were strongly correlated ($r = 0.939$). These findings suggest that, if skull bone volume determinations could safely become available in alcohol-exposed and non-exposed children, the neurocranium bone volume would be a more accurate predictor of prenatal alcohol exposure than either facial dysmorphology or head circumference.

Although CT scanning of the head is not without risk and segmentation of the skull bones may be clinically demanding, quantitative CT scans eventually could provide better identification of prenatal alcohol exposure in clinical screening of children at risk for FASD. The lack of age-specific norms for cranial bone volumes and the potential risk of unnecessary radiation exposure with elective use of CT in children currently limit application of this approach in helping identify children with FASD. While it may be possible to build a reasonably large normative data base from CT scans in children undergoing head CT for medical purposes, perhaps it is more difficult to justify non-diagnostic CT scans for FASD (or other) children. Nevertheless, research and development efforts in biomedical imaging are improving safety by lowering scan times and creating new technology that reduces radiation exposure. For example, electron-beam CT is a relatively new technology. A study in children found that multi-detector CT delivered higher doses of radiation compared with the doses delivered in electron-beam CT (Hunold et al., 2003). In time, as electron-beam CT and other technology becomes more clinically available, it is reasonable to expect that the safety of CT will sufficiently outweigh the risks and that the quantitative approaches used in this study will become clinically feasible on a routine basis.

Prenatal alcohol exposure significantly affected all three of the neurocranium bones (frontal, parietal, and occipital) and four of the five viscerocranium bones (maxilla, mandible,

lacrimal, jugal, but not nasal). Overall, the bone volume changes were highly correlated, such that in the analysis using total skull bone volume as a covariate, none of the individual bone volumes remained significant. However, the neurocranium bone volumes were generally better predictors of prenatal alcohol exposure in the discriminant analysis, and only the parietal and occipital bones distinguished the HBA group after the effects of cranial circumference were statistically removed. The neurocranium bones are directly and anatomically related to the three skull distance measures (upper facial depth, bitragal width, interorbital distance) and one facial measure (inner canthal width) that were significantly reduced in the binge and heavy binge alcohol treatments. Thus, it appears that prenatal binge alcohol exposure effects on head and skull measures may be more directly related to growth of the neurocranium than the viscerocranium, and relative to routine FAS screening measures, alcohol-induced reductions in the neurocranium volumes may provide better detection of prenatal alcohol exposure.

In comparing the two binge alcohol exposure treatments, no significant differences were evident in any of the volumetric or linear distances in the BA and HBA treatments in the absence of covariance analysis. The two alcohol treatments used in this “weekend binge drinking” model of the first 8 weeks of human pregnancy both produced relatively high peak blood alcohol concentrations (199 and 280 mg/dL, respectively). Both alcohol treatments were equally prone to produce skull volume and craniofacial changes. The 1.75 g/kg per day dose was sufficient to induce craniofacial abnormalities. The only differences identified in the BA and HBA treatments were from the covariance analysis (with cranial circumference and sex as covariates), which statistically controlled for overall effects of head size. In that analysis, the HBA treatment produced significantly greater reductions than the BA treatment in the adjusted means of the occipital bone volume. The occipital bone was also the most accurate predictor in distinguishing between the BA and HBA treatments in the discriminant analysis. This suggests that the occipital bone volume may be a sensitive biomarker for increasing severity of binge drinking during the first trimester.

In terms of craniofacial distance measures, reductions in three of the nine bone distances (upper facial depth, bitragal width, interorbital distance) and one of the ten soft-tissue face distances (inner canthal width) distinguished BA and HBA lambs from NC and SC lambs. All four measures were highly correlated with cranial circumference. When cranial circumference was used as a covariate, none of the measures remained significant between the BA and HBA groups and the NC and SC groups. The interorbital distance predicted the alcohol-exposed treatments from the control treatments with 93.8–100% accuracy (87.5–100% sensitivities and 93.8–100% specificities), and the inner canthal width was 90–100% accurate (87.5–100% sensitivities and 75–100% specificities). There were significant correlations between several facial measures and the underlying bone measures that were closely associated with those facial features. Significant reductions in the correlated measures of interorbital distance (bone) and inner canthal width (face), as well as the high accuracy in classifying prenatal alcohol treatment based on interorbital distance and on inner canthal width, suggests that these two measures (associated with reduced distances between the eyes) may also help identify children with FASD. These findings are the first report of quantitative skull and facial morphometric changes in the sheep model of maternal binge alcohol exposure during a portion of the first trimester equivalent.

A previous rodent study analyzed facial measurements on embryonic day 17 C57BL/6N mice and found significant treatment effects in 12 of the 15 measures analyzed. Four measures (upper face, mid-face, nasal length, nasal bridge) identified the alcohol group from the pair and chow-fed groups (Anthony et al., 2010), which showed only partial correspondence to the four measures identified in this sheep study (upper facial depth, bitragal width, interorbital distance, and inner canthal width). Differences between the mouse model and sheep model outcomes could be explained either by differences in 1) alcohol exposure models (with the sheep model involving a more direct experimental control over binge-like exposure), 2) the older developmental status of the sheep (peripubertal lambs compared to late-fetal mice), or 3) species differences between sheep and rodents in how alcohol alters craniofacial development.

A comparable CT study of skull morphology was conducted in 21-day-old C57BL/6J mice that showed bone volumes were capable of identifying alcohol-exposed offspring (Shen et al., 2013), similar to findings in this study. The mouse model studies, involving maternal consumption of alcohol liquid diets, produce prenatal and postnatal growth deficits in offspring that can be conflated with craniofacial bone growth deficits. In this sheep model paradigm, there were no significant effects on birth weight or postnatal growth of the lambs.

Palpebral fissure length is a cardinal feature to assess FAS in children (Astley, 2006; Bertrand et al., 2005; Chudley et al., 2005; Jones & Smith, 1973), yet palpebral fissure length was not reliably affected in this sheep model of prenatal alcohol exposure, and it was not significantly correlated with cranial circumference or total skull bone volume. The results of this study indicate that neither the orbital height, orbital width (bone), or the palpebral fissure length (face) were significantly different between alcohol-exposed and control lambs. This contrasts with a human study in which significant reductions were found in palpebral fissure length, inner canthal width, and outer canthal width (Moore et al., 2007). A recent human study concluded that palpebral fissure length and head circumference are independent of each other and that short palpebral fissures are likely reduced due to forebrain damage, not necessarily due to smaller head size (Jones et al., 2009). In the embryonic mouse model, a direct correlation was identified between reduced palpebral fissure length and reduced globe size as well as forebrain reduction implicating a correlation to forebrain damage (Parnell et al., 2006). Palpebral fissure length in this sheep model was not useful in distinguishing between the four treatment groups. In contrast and consistent with the human study by Moore and colleagues, the sheep model did find significant alcohol-induced reductions in the inner canthal width relative to controls (NC; SC), and the outer canthal width was significantly reduced relative to the SC group. This suggests that in the sheep model, craniofacial effects are more prominent in measures linked to craniofacial and skull width development (inner and outer canthal widths, interorbital widths, bitragal width, upper facial depth) rather than direct orbital measures. These differences may reflect species differences in response to alcohol exposure, or they may point to a previously unrecognized sensitivity of mid-facial width measurements in FASD screening. The Moore et al. study (2007) also included a wide range of ages, an ethnically diverse population, and unknown maternal drinking history. These sources of variance may have important influences on craniofacial morphometry.

There are many translational advantages of the sheep model of FASD (Cudd, 2005), in which dose, pattern, and timing of alcohol exposure are experimentally controlled. The resulting blood alcohol concentrations are known and these underscore the translational importance of the current findings that identify neurocranium bone volumes as a potential biomarker of prenatal alcohol exposure. Sheep model studies are limited by several factors that make it difficult to get large sample sizes and adequate sex representation for experiments. Studies take longer to complete, are more labor intensive, and are more expensive than rodent studies. Despite these limitations, experimental studies can be done utilizing the sheep model in a translational role for preclinical studies of FASD. This is due to improved ability in controlling and matching the experimental conditions of daily patterns, developmental timing of alcohol exposure more similar to humans, and the development of measures to advance diagnostic phenotypes of FASD. Sheep have body weights and head/brain sizes that are more comparable to humans and they have long gestational periods (147 days) closely resembling human gestation (280 days). Sheep also have brain development stages *in utero* that can be matched more directly to prenatal brain development in humans (Cudd, 2005). Findings in this study illustrate the translational value of the sheep model, confirming that the effects on bone volumes are replicable in multiple species, but also provide novel evidence that neurocranium bone volumes may provide an optimal structural biomarker of the effects of first trimester binge drinking associated with FASD.

To summarize, these results confirmed our hypothesis that CT morphometric analysis is an effective tool for detecting prenatal binge alcohol exposure in lambs. Lambs born to ewes exposed to alcohol during the period of embryonic development comparable to the first 8 weeks of human pregnancy had reduced CT-derived volumetrics of the bones and, less reliably, reduced facial and skull measures. Discriminant analysis of CT measures could identify alcohol-exposed from non-exposed lambs with 100% accuracy. These changes correlate to reduced craniofacial bone volumes in the rodent model and reduced head circumference in both rodents and humans. Facial measurements in the sheep share some similarities in humans with FAS, including reductions in the upper facial depth, bitragal width, and inner canthal distance, but other dysmorphic effects seen in humans were not reliably produced in this sheep model (palpebral fissure width).

Several findings in this study highlight the potential translational value of the sheep model and the development of better diagnostic tools for craniofacial phenotypes of FASD. To the extent that CT scans can become feasible in FASD research settings, the findings in this study predict several relatively straightforward measures that should accurately identify otherwise non-dysmorphic children who experienced binge-like alcohol exposure during the first trimester. The best predictors would most likely be segmented bone volumes of the neurocranium (frontal, parietal, occipital, or volume of the total skull). These measures should have high sensitivity and specificity in classifying prenatal binge-alcohol exposed children from non-exposed children. Inclusion of the occipital bone volume may also help determine which children were heavily exposed during the first trimester (likely to include those diagnosed with FAS). Concurrent use of multiple quantitative CT measures (e.g., neurocranium bone volumes together with cranial circumference, interorbital distance, and

inner canthal width) may further improve the reliability of classification. Implementation of CT morphometrics would also require establishment of age-specific normative data. The degree to which these bone structural phenotypes (observed in this study in peripubertal sheep) might change over development is not known, and whether they could be applied to earlier ages (childhood) or later ages (adolescence or young adulthood) remains to be determined. The implication is that development of comparative CT analysis may significantly improve the identification of children with FASD, individuals whose status otherwise would be either unknown, uncertain, or overlooked.

Acknowledgments

This study was supported by Texas A&M CVM Post-Doctoral Grant (SMB) and NIAAA Grant AA017120 and AA18166-2 (SW). This work was done in conjunction with the Collaborative Initiative on Fetal Alcohol Spectrum Disorders (CIFASD), which is funded by grants from the National Institute on Alcohol and Alcohol Abuse (NIAAA). Additional information about CIFASD can be found at www.cifasd.org. Those participating in this study wish to acknowledge the primary and important role of the late Dr. Timothy Cudd in designing and initiating this work.

References

Aase JM, Jones KL, Clarren SK. Do we need the term “FAE”? Pediatrics. 1995; 95:428–430. [PubMed: 7862486]

Anthony B, Vinci-Booher S, Wetherill L, Ward R, Goodlett C, Zhou FC. Alcohol-induced facial dysmorphology in C57BL/6 mouse models of fetal alcohol spectrum disorder. Alcohol. 2010; 44:659–671. [PubMed: 20570474]

Astley SJ. Comparison of the 4-digit diagnostic code and the Hoyme diagnostic guidelines for fetal alcohol spectrum disorders. Pediatrics. 2006; 118:1532–1545. [PubMed: 17015544]

Astley SJ, Clarren SK. Diagnosing the full spectrum of fetal alcohol-exposed individuals: introducing the 4-digit diagnostic code. Alcohol and Alcoholism. 2000; 35:400–410. [PubMed: 10906009]

Bertrand J, Floyd LL, Weber MK. Guidelines for identifying and referring persons with fetal alcohol syndrome. MMWR Recommendations and Reports. 2005; 54:1–14. [PubMed: 16251866]

Carter RC, Jacobson JL, Sokol RJ, Avison MJ, Jacobson SW. Fetal alcohol-related growth restriction from birth through young adulthood and moderating effects of maternal prepregnancy weight. Alcoholism: Clinical and Experimental Research. 2013; 37:452–462.

Cartwright MM, Smith SM. Increased cell death and reduced neural crest cell numbers in ethanol-exposed embryos: partial basis for the fetal alcohol syndrome phenotype. Alcoholism: Clinical and Experimental Research. 1995; 19:378–386.

CDC. Alcohol use among pregnant and nonpregnant women of childbearing age –United States, 1991–2005. MMWR Morbidity and Mortality Weekly Report. 2009; 58:529–532. [PubMed: 19478721]

CDC. Alcohol use and binge drinking among women of childbearing age--United States, 2006–2010. MMWR Morbidity and Mortality Weekly Report. 2012; 61:534–538. [PubMed: 22810267]

Chudley AE, Conry J, Cook JL, Loock C, Rosales T, LeBlanc N. Fetal alcohol spectrum disorder: Canadian guidelines for diagnosis. Canadian Medical Association Journal. 2005; 172(5 Suppl):S1–S21. [PubMed: 15738468]

Conover EA, Jones KL. Safety concerns regarding binge drinking in pregnancy: a review. Birth Defects Research Part A, Clinical and Molecular Teratology. 2012; 94:570–575.

Cudd TA. Animal model systems for the study of alcohol teratology. Experimental Biology and Medicine (Maywood). 2005; 230:389–393.

Hernandez-Guerrero JC, Ledesma-Montes C, Loyola-Rodriguez JP. Effects of maternal ethanol intake on second alcoholic generation murine skull and mandibular size. Archives of Medical Research. 1998; 29:297–302. [PubMed: 9887546]

Hoyme HE, May PA, Kalberg WO, Kodituwakku P, Gossage JP, Trujillo PM, et al. A practical clinical approach to diagnosis of fetal alcohol spectrum disorders: clarification of the 1996 institute of medicine criteria. Pediatrics. 2005; 115:39–47. [PubMed: 15629980]

Hunold P, Vogt FM, Schmermund A, Debatin JF, Kerkhoff G, Budde T, et al. Radiation exposure during cardiac CT: effective doses at multi-detector row CT and electron-beam CT. Radiology. 2003; 226:145–152. [PubMed: 12511683]

Jones KL, Hoyme HE, Robinson LK, del Campo M, Manning MA, Bakhireva LN, et al. Developmental pathogenesis of short palpebral fissure length in children with fetal alcohol syndrome. Birth Defects Research Part A, Clinical and Molecular Teratology. 2009; 85:695–699.

Jones KL, Hoyme HE, Robinson LK, Del Campo M, Manning MA, Prewitt LM, et al. Fetal alcohol spectrum disorders: Extending the range of structural defects. American Journal of Medical Genetics Part A. 2010; 152A:2731–2735. [PubMed: 20949507]

Jones KL, Smith DW. Recognition of the fetal alcohol syndrome in early infancy. Lancet. 1973; 302:999–1001. [PubMed: 4127281]

Kaminen-Ahola N, Ahola A, Maga M, Mallitt KA, Fahey P, Cox TC, et al. Maternal ethanol consumption alters the epigenotype and the phenotype of offspring in a mouse model. PLoS Genetics. 2010; 6:e1000811. [PubMed: 20084100]

Leibson T, Neuman G, Chudley AE, Koren G. The differential diagnosis of fetal alcohol spectrum disorder. Journal of Population Therapeutics and Clinical Pharmacology. 2014; 21:e1–e30. [PubMed: 24639410]

Lipinski RJ, Hammond P, O'Leary-Moore SK, Ament JJ, Pecevich SJ, Jiang Y, et al. Ethanol-induced face-brain dysmorphology patterns are correlative and exposure-stage dependent. PLoS One. 2012; 7:e43067. [PubMed: 22937012]

Lupton C, Burd L, Harwood R. Cost of fetal alcohol spectrum disorders. American Journal of Medical Genetics Part C, Seminars in Medical Genetics. 2004; 127C:42–50.

Maier SE, West JR. Drinking patterns and alcohol-related birth defects. Alcohol Research & Health. 2001; 25:168–174. [PubMed: 11810954]

May PA, Gossage JP, Kalberg WO, Robinson LK, Buckley D, Manning M, et al. Prevalence and epidemiologic characteristics of FASD from various research methods with an emphasis on recent in-school studies. Developmental Disabilities Research Reviews. 2009; 15:176–192. [PubMed: 19731384]

The Merck Veterinary Manual. Whitehouse Station, NJ: Merck & Co; 2005.

Moore ES, Ward RE, Wetherill LF, Rogers JL, Autti-Rämö I, Fagerlund A, et al. Unique facial features distinguish fetal alcohol syndrome patients and controls in diverse ethnic populations. Alcoholism: Clinical and Experimental Research. 2007; 31:1707–1713.

Moore, KL. The developing human: clinically oriented embryology. Philadelphia, PA: Saunders/ Elsevier; 2013.

NIAAA. NIH statement on International FASD Awareness Day [Press release]. 2012. Retrieved from http://www.niaaa.nih.gov/news-events/news-releases/nih-statement-international-fasd-awareness-day

O'Rahilly, R.; Müller, F. Human embryology and teratology. 2nd. New York, NY: Wiley-Liss; 1996.

Ortega-García JA, Gutierrez-Churango JE, Sánchez-Sauco MF, Martínez-Aroca M, Delgado-Marín JL, Sánchez-Solis M, et al. Head circumference at birth and exposure to tobacco, alcohol and illegal drugs during early pregnancy. Child's Nervous System. 2012; 28:433–439.

Parnell SE, Dehart DB, Wills TA, Chen SY, Hodge CW, Besheer J, et al. Maternal oral intake mouse model for fetal alcohol spectrum disorders: ocular defects as a measure of effect. Alcoholism: Clinical and Experimental Reserch. 2006; 30:1791–1798.

Ramadoss J, Hogan HA, Given JC, West JR, Cudd TA. Binge alcohol exposure during all three trimesters alters bone strength and growth in fetal sheep. Alcohol. 2006; 38:185–192. [PubMed: 16905445]

Reynolds ML, Møllgård K. The distribution of plasma proteins in the neocortex and early allocortex of the developing sheep brain. Anatomy and Embryology. 1985; 171:41–60. [PubMed: 3985357]

Riley EP, McGee CL. Fetal alcohol spectrum disorders: an overview with emphasis on changes in brain and behavior. Experimental Biology and Medicine, (Maywood). 2005; 230:357–365.

Robin NH, Zackai EH. Unusual craniofacial dysmorphia due to prenatal alcohol and cocaine exposure. Teratology. 1994; 50:160–164. [PubMed: 7801303]

Rovasio RA, Battiato NL. Role of early migratory neural crest cells in developmental anomalies induced by ethanol. The International Journal of Developmental Biology. 1995; 39:421–422. [PubMed: 7669554]

Schmidt EJ, Parsons TE, Jamniczky HA, Gitelman J, Trpkov C, Boughner JC, et al. Micro-computed tomography-based phenotypic approaches in embryology: procedural artifacts on assessments of embryonic craniofacial growth and development. BMC Developmental Biology. 2010; 10:18. [PubMed: 20163731]

Shen L, Ai H, Liang Y, Ren X, Anthony CB, Goodlett CR, et al. Effect of prenatal alcohol exposure on bony craniofacial development: a mouse MicroCT study. Alcohol. 2013; 47:405–415. [PubMed: 23809873]

Smith SM. Alcohol-induced cell death in the embryo. Alcohol Health and Research World. 1997; 21:287–297. [PubMed: 15706739]

Smith SM, Garic A, Flentke GR, Berres ME. Neural crest development in fetal alcohol syndrome. Birth Defects Research Part C, Embryo Today: Reviews. 2014; 102:210–220.

Sokol RJ, Clarren SK. Guidelines for use of terminology describing the impact of prenatal alcohol on the offspring. Alcoholism: Clinical and Experimental Research. 1989; 13:597–598.

Streissguth AP. A Long-Term Perspective of FAS. Alcohol Health & Research World. 1994; 18:8.

Streissguth AP, Aase JM, Clarren SK, Randels SP, LaDue RA, Smith DF. Fetal alcohol syndrome in adolescents and adults. JAMA. 1991; 265:1961–1967. [PubMed: 2008025]

Sulik KK. Craniofacial defects from genetic and teratogen-induced deficiencies in presomite embryos. Birth Defects Original Article Series. 1984; 20:79–98. [PubMed: 6542431]

Sulik KK, Cook CS, Webster WS. Teratogens and craniofacial malformations: relationships to cell death. Development. 1988; 103 Suppl:213–231. [PubMed: 3074910]

Washburn SE, Sawant OB, Lunde ER, Wu G, Cudd TA. Acute alcohol exposure, acidemia or glutamine administration impacts amino acid homeostasis in ovine maternal and fetal plasma. Amino Acids. 2013; 45:543–554. [PubMed: 23315157]

Wattendorf DJ, Muenke M. Fetal alcohol spectrum disorders. American Family Physician. 2005; 72:279–282. 285. [PubMed: 16050451]

Highlights

- CT-derived craniofacial bone volumes and measurements detect alcohol-exposed lambs
- Alcohol-exposed lambs have reduced cranial circumference and total skull bone volume
- Alcohol-exposed lambs have reduced volumes in segmented skull bones (7 out of 8)
- Alcohol-exposed lambs have decreased craniofacial measures (4 out of 19)
- Occipital bone volume distinguishes binge exposure from heavy binge exposure lambs
- CT has diagnostic potential for quantitating facial dysmorphology in FASD

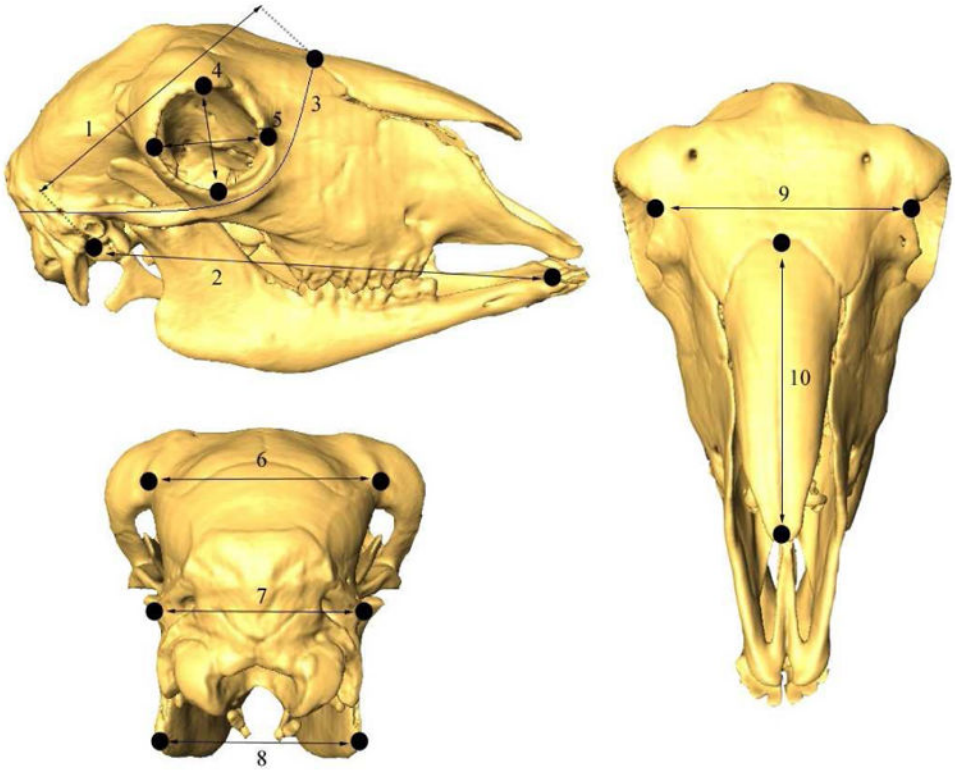

Fig. 1.

Normal control lamb skull (lateral, caudal, and dorsal 3D aspects shown) as visualized with Amira Software (Visage Imaging, Inc., San Diego, CA). The 10 skull linear measurements obtained from each of the lamb skulls are shown as identified in Table 1.

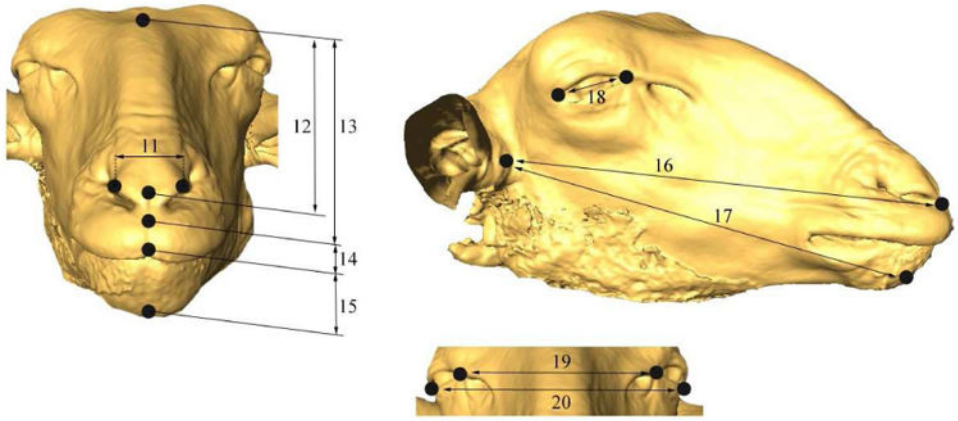

Fig. 2.

Normal control lamb face (rostral and lateral 3D aspects shown) as visualized with Amira Software (Visage Imaging, Inc., San Diego, CA). The 10 face linear measurements obtained from each lamb are shown as identified in Table 1. The ears have been cropped from the image.

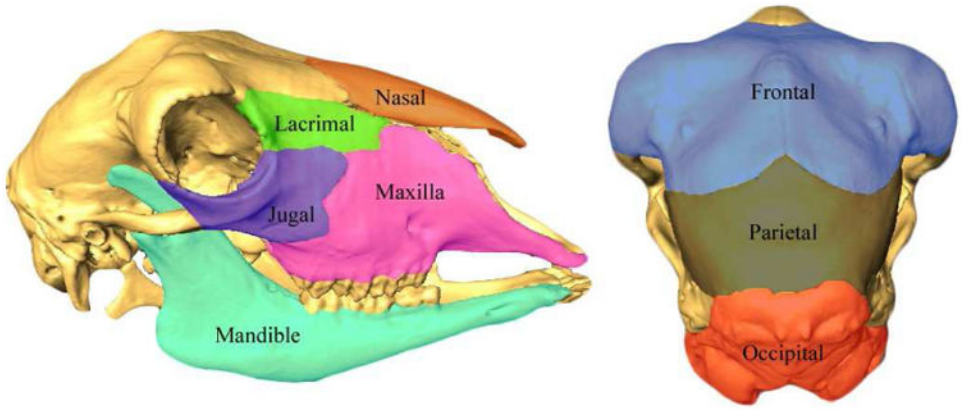

Fig. 3.

Normal control lamb skull (lateral and caudal 3D aspects shown) as visualized with Amira Software (Visage Imaging, Inc., San Diego, CA). The 8 bones segmented for bone volumes on each lamb skull are shown. In the lateral view, only the right-sided segmentation is visible. Total skull bone volume was calculated by adding together the volume of all of the bone segmentations (left and right sides).

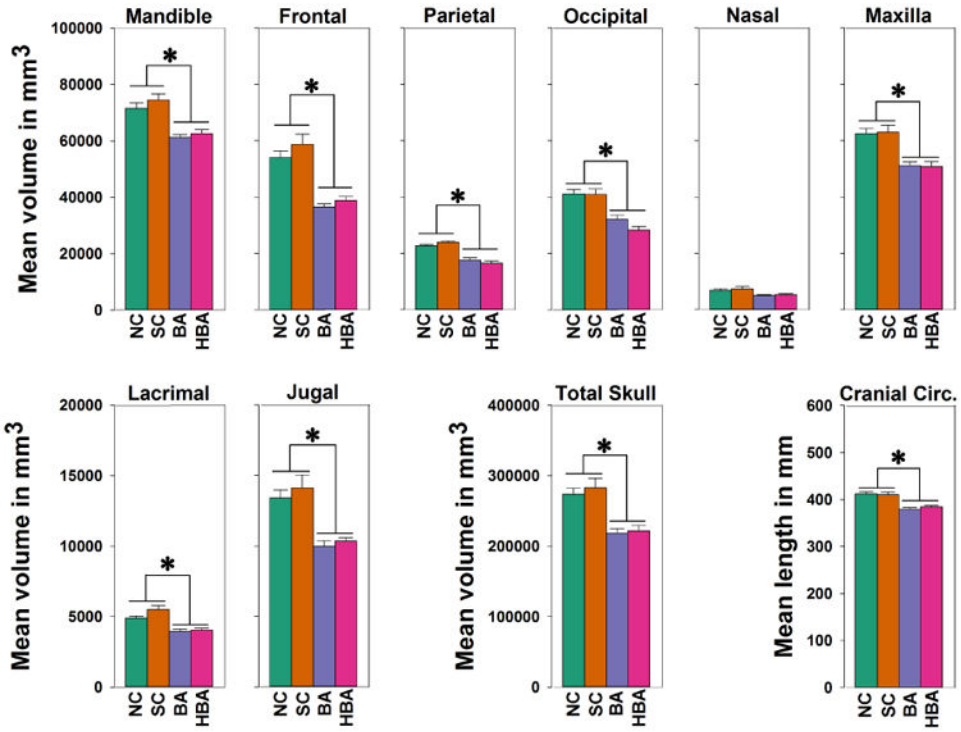

Fig. 4.

Treatment effects on 9 volumetric skull measures and the cranial circumference measure. The y-axis indicates the mean volume (± SEM) in mm^3 for the 8 segmented bone volumes and total skull volume, or length (in mm) for cranial circumference. Note the scale for the 6 bones in the top panels (maximum of 100,000 mm^3) differs from that in the lower panels for the lacrimal and jugal bones (maximum of 20,000 mm^3). For the bone volumes, the ANOVA α level was adjusted to 0.0056 (=0.05/9) for the nine ANOVAs performed, followed by the Holm-Sidak method for pairwise comparisons ($p < 0.05$). For cranial circumference, the ANOVA α level was 0.05, followed by the Holm-Sidak method for pairwise comparisons ($p < 0.05$). Significant group differences are indicated within each panel. An asterisk (*) indicates that the volumes of two control groups (NC and SC) were significantly greater than the two alcohol-exposed groups (BA and HBA); NC and SC did not differ from each other, and BA and HBA did not differ from each other.

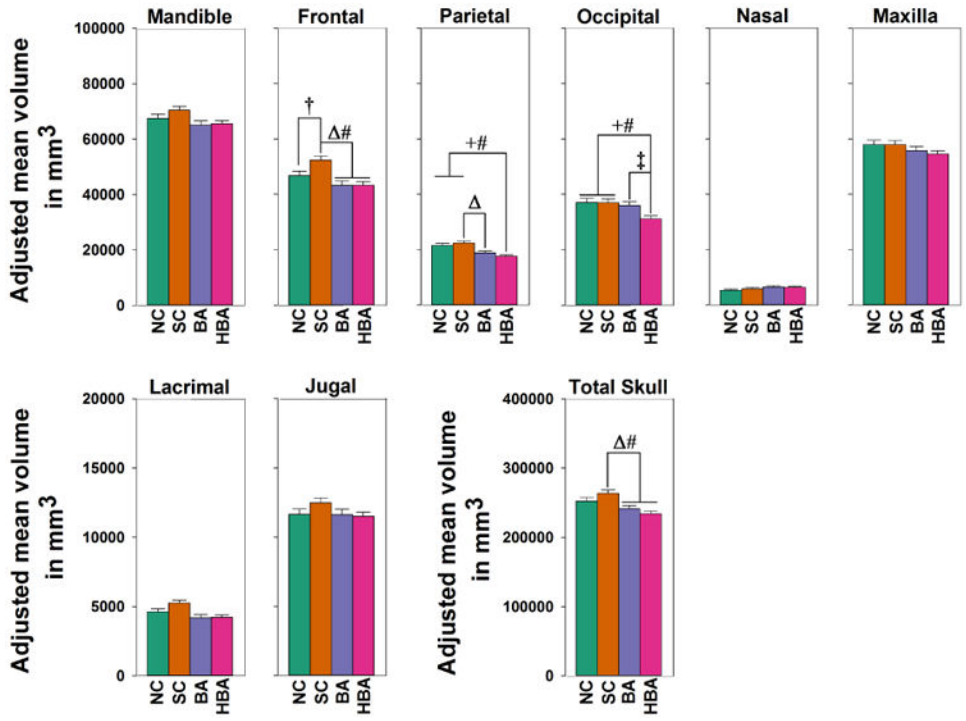

Fig. 5.

Treatment effects on 9 volumetric skull measures while controlling for cranial circumference and sex, showing the adjusted group means (± SEM) after removal of the influence of the two covariates. The y-axis indicates the adjusted volume in mm^3 for the 9 measures (note scale differences between the top and bottom panels). For bone volumes, the ANOVA α level was adjusted to 0.0056 (=0.05/9) for the nine ANOVAs performed, followed by the Holm-Sidak method for pairwise comparisons ($p < 0.05$). For cranial circumference, the ANOVA α level was 0.05, followed by the Holm-Sidak method for pairwise comparisons ($p < 0.05$). Significant group differences are indicated within each panel. Note that after controlling for effects of differences in cranial circumference, the effects of the heavy binge alcohol (HBA) treatment relative to controls were still detectable in the parietal and occipital bone volumes, and the HBA even differed from the BA group in the occipital bone volume. Significance between NC vs. SC is indicated with a dagger sign (†), BA vs. SC is indicated with a delta sign (Δ), HBA vs. SC is indicated with a pound sign (#), HBA vs. NC is indicated with a plus sign (+), and HBA vs. BA is indicated with a double dagger sign (‡).

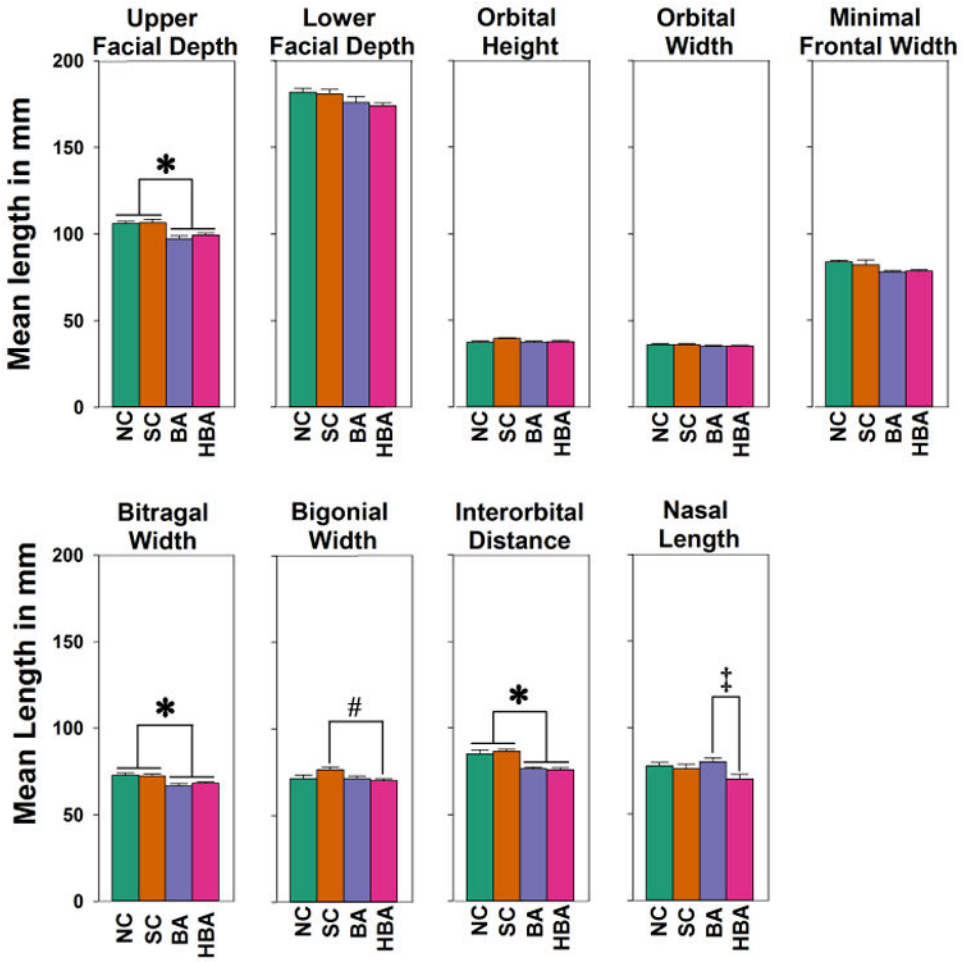

Fig. 6.

Treatment effects on 9 skull distance measures. The y-axis indicates the mean length (± SEM) in mm. The ANOVA α level was adjusted to 0.0056 (=0.05/9) for the nine ANOVAs performed, followed by the Holm-Sidak method for pairwise comparisons ($p < 0.05$). Significant group differences are indicated within each panel. An asterisk (*) indicates significance between the following four pairs: BA vs. NC, HBA vs. NC, BA vs. SC, and HBA vs. SC. Significance between HBA vs. SC is indicated with a pound sign (#) and significance between HBA vs. BA is indicated with a double dagger sign (‡).

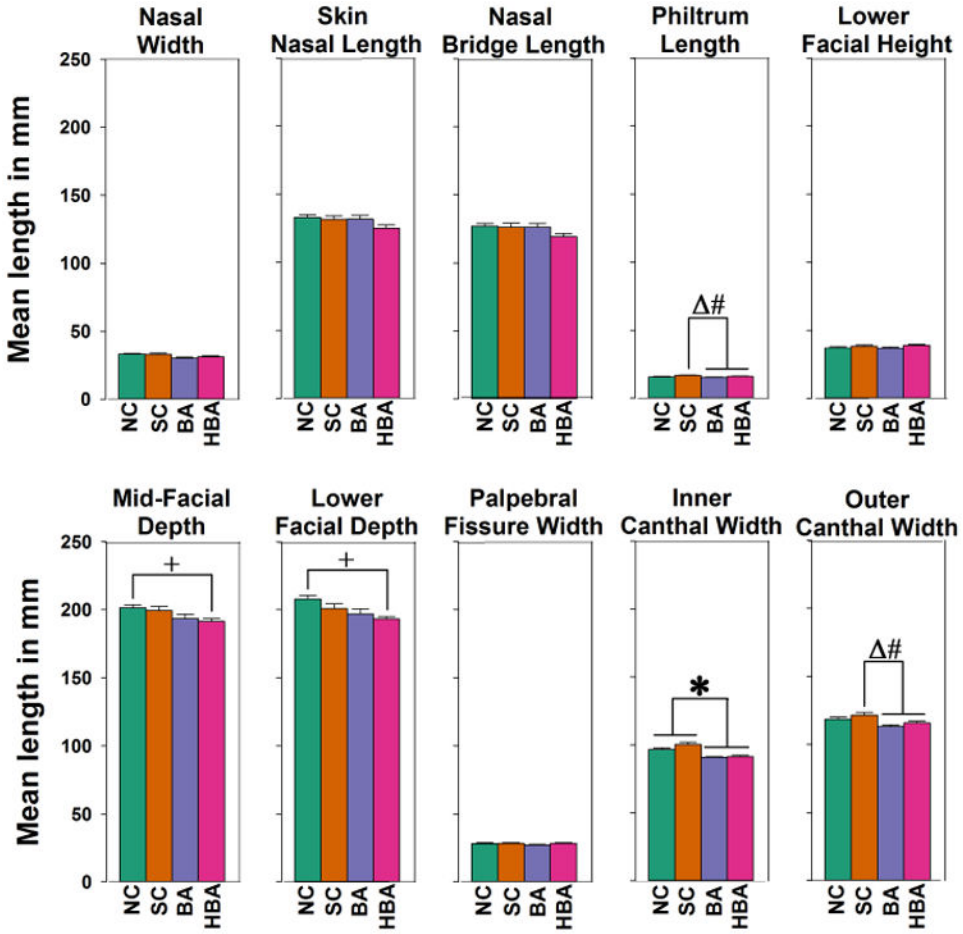

Fig. 7.

Treatment effects on 10 face distance measures. The y-axis indicates the mean length (± SEM) in mm. The ANOVA α level was adjusted to 0.005 (=0.05/10) for the ten ANOVAs performed, followed by the Holm-Sidak method for pairwise comparisons ($p < 0.05$). Significant group differences are indicated within each panel. An asterisk (*) indicates significance between the following four pairs: BA vs. NC, HBA vs. NC, BA vs. SC, and HBA vs. SC. Significance between BA vs. SC is indicated with a delta sign (Δ), HBA vs. SC is indicated with a pound sign (#), and HBA vs. NC is indicated with a plus sign (+).

Table 1

Craniofacial measurements and landmarks.

Fig.	Location	Number	Measurement
1	Skull	1	Upper facial depth[a]
		2	Lower facial depth[a]
		3	Cranial circumference
		4	Orbital height[a]
		5	Orbital width[a]
		6	Minimal frontal width
		7	Bitragal width
		8	Bigonial width
		9	Interorbital distance
		10	Nasal length
2	Face	11	Nasal width
		12	Nasal length
		13	Nasal bridge length
		14	Philtrum length
		15	Lower facial height
		16	Mid-facial depth[a]
		17	Lower facial depth[a]
		18	Palpebral fissure length[a]
		19	Inner canthal width
		20	Outer canthal width

Numbers are keyed to Figs. 1 and 2.

[a]Both right and left side measurements were taken.

Table 2

Pearson correlation coefficients among the 9 volumetric skull measures and the cranial circumference measure

	Occipital	Parietal	Frontal	Nasal	Lacrimal	Jugal	Maxilla	Mandible	Total Skull	Cranial Circ
Occipital	**1.000**	**0.892**	**0.828**	**0.729**	**0.775**	**0.850**	**0.874**	**0.821**	**0.931**	**0.847**
Parietal	**0.892**	**1.000**	**0.850**	**0.640**	**0.799**	**0.817**	**0.849**	**0.794**	**0.912**	**0.821**
Frontal	**0.828**	**0.850**	**1.000**	**0.804**	**0.843**	**0.916**	**0.871**	**0.836**	**0.955**	**0.918**
Nasal	**0.729**	**0.640**	**0.804**	**1.000**	**0.693**	**0.778**	**0.771**	**0.686**	**0.811**	**0.801**
Lacrimal	**0.775**	**0.799**	**0.843**	**0.693**	**1.000**	**0.785**	**0.798**	**0.650**	**0.838**	**0.716**
Jugal	**0.850**	**0.817**	**0.916**	**0.778**	**0.785**	**1.000**	**0.904**	**0.894**	**0.952**	**0.928**
Maxilla	**0.874**	**0.849**	**0.871**	**0.771**	**0.798**	**0.904**	**1.000**	**0.839**	**0.950**	**0.882**
Mandible	**0.821**	**0.794**	**0.836**	**0.686**	**0.650**	**0.894**	**0.839**	**1.000**	**0.915**	**0.869**
Total Skull	**0.931**	**0.912**	**0.955**	**0.811**	**0.838**	**0.952**	**0.950**	**0.915**	**1.000**	**0.939**
Cranial Circ	**0.847**	**0.821**	**0.918**	**0.801**	**0.716**	**0.928**	**0.882**	**0.869**	**0.939**	**1.000**

All correlations are in bold, indicating correlations are significant at $p < 0.001$ for all measures.

Table 3

Pearson correlation coefficients among the 9 skull distance measures and the cranial circumference

	Upper Facial Depth	Lower Facial Depth	Orbital Height	Orbital Width	Minimal Frontal Width	Bitragal Width	Bigonial Width	Interorbital Distance	Skull Nasal Length	Cranial Circ
Upper Facial Depth	**1.000**	**0.721**	**0.569**	0.259	**0.546**	**0.730**	0.323	**0.606**	0.110	**0.823**
Lower Facial Depth	**0.721**	**1.000**	**0.665**	0.256	0.468	**0.677**	0.513	**0.569**	**0.595**	**0.812**
Orbital Height	**0.569**	**0.665**	**1.000**	0.469	0.217	**0.531**	**0.583**	**0.530**	0.433	**0.605**
Orbital Width	0.259	0.256	0.469	**1.000**	0.374	0.496	0.246	0.402	0.046	0.462
Minimal Frontal Width	**0.546**	0.468	0.217	0.374	**1.000**	**0.681**	0.429	**0.581**	0.157	**0.754**
Bitragal Width	**0.730**	**0.677**	**0.531**	0.496	**0.681**	**1.000**	**0.566**	**0.783**	0.178	**0.897**
Bigonial Width	0.323	0.513	**0.583**	0.246	0.429	**0.566**	**1.000**	**0.623**	0.414	**0.579**
Interorbital Distance	**0.606**	**0.569**	**0.530**	0.402	**0.581**	**0.783**	**0.623**	**1.000**	0.286	**0.780**
Skull Nasal Length	0.110	**0.595**	0.433	0.046	0.157	0.178	0.414	0.286	**1.000**	0.382
Cranial Circ	**0.823**	**0.812**	**0.605**	0.462	**0.754**	**0.897**	**0.579**	**0.780**	0.382	**1.000**

Correlations in bold are significant at $p < 0.001$.

Table 4

Pearson correlation coefficients among the 10 face distance measures and the cranial circumference measure

	Nasal Width	Facial Nasal Length	Nasal Bridge Length	Philtrum Length	Lower Facial Height	Mid-Facial Depth	Lower Facial Depth	Palpebral Fissure Length	Inner Canthal Width	Outer Canthal Width	Cranial Circ
Nasal Width	**1.000**	**0.631**	**0.576**	**0.634**	0.517	**0.717**	0.502	0.318	**0.606**	0.463	**0.728**
Facial Nasal Length	**0.631**	**1.000**	**0.977**	0.404	0.247	**0.817**	**0.527**	0.0583	0.488	0.259	**0.582**
Nasal Bridge Length	**0.576**	**0.977**	**1.000**	0.396	0.197	**0.767**	0.497	−0.0136	0.490	0.251	**0.544**
Philtrum Length	**0.634**	0.404	0.396	**1.000**	**0.624**	0.506	0.337	0.241	**0.554**	**0.547**	**0.543**
Lower Facial Height	0.517	0.247	0.197	**0.624**	**1.000**	0.413	0.0809	0.325	0.378	0.364	0.382
Mid-Facial Depth	**0.717**	**0.817**	**0.767**	0.506	0.413	**1.000**	**0.758**	0.199	**0.643**	0.463	**0.822**
Lower Facial Depth	0.502	**0.527**	0.497	0.337	0.0809	**0.758**	**1.000**	0.141	**0.579**	0.460	**0.754**
Palpebral Fissure Length	0.318	0.0583	−0.0136	0.241	0.325	0.199	0.141	**1.000**	0.144	0.288	0.222
Inner Canthal Width	**0.606**	0.488	0.490	**0.554**	0.378	**0.643**	**0.579**	0.144	**1.000**	**0.836**	**0.837**
Outer Canthal Width	0.463	0.259	0.251	**0.547**	0.364	0.463	0.460	0.288	**0.836**	**1.000**	**0.724**
Cranial Circ	**0.728**	**0.582**	**0.544**	**0.543**	0.382	**0.822**	**0.754**	0.222	**0.837**	**0.724**	**1.000**

Correlations in bold are significant at $p < 0.001$.

Table 5

Pearson correlation coefficients among the 10 face distance measures and 9 skull distance measures

	Nasal Width	Face Nasal Length	Nasal Bridge Length	Philtrum Length	Lower Facial Height	Mid-Facial Depth	Lower Facial Depth	Palpebral Fissure Length	Inner Canthal Width	Outer Canthal Width
Upper Facial Depth	**0.534**	0.320	0.311	0.523	0.357	**0.745**	**0.668**	0.213	**0.660**	**0.556**
Lower Facial Depth	**0.674**	**0.760**	**0.697**	0.505	0.288	**0.952**	**0.812**	0.117	**0.617**	0.510
Orbital Height	0.507	0.467	0.483	**0.537**	0.293	0.494	0.385	0.380	0.512	0.446
Orbital Width	0.314	0.062	0.078	0.377	0.197	0.322	0.484	0.465	0.483	0.517
Minimal Frontal Width	0.295	0.288	0.274	0.305	0.210	**0.532**	0.523	−0.013	**0.705**	**0.673**
Bitragal Width	**0.605**	0.379	0.317	0.478	0.330	**0.687**	**0.594**	0.191	**0.761**	**0.753**
Bigonial Width	0.494	0.495	0.488	0.445	0.244	0.482	0.240	0.075	**0.675**	**0.691**
Interorbital Distance	**0.533**	0.418	0.430	0.409	0.143	**0.588**	0.507	0.059	**0.813**	**0.694**
Skull Nasal Length	0.467	**0.919**	**0.920**	0.322	0.247	**0.808**	0.437	0.071	0.349	0.126

Correlations in bold are significant at $p < 0.001$.

Table 6A

Results of univariate ROC analysis: areas under ROC curve (AUCs) are shown for (a) skull bone volumetric measurements and cranial circumference.

	No Covariates					
(a) Bone	**BA vs NC**	**HBA vs NC**	**BA vs SC**	**HBA vs SC**	**NC vs SC**	**HBA vs BA**
Mandible	**1**	**1**	**1**	**1**	0.734	0.656
Frontal	**1**	**1**	**1**	**1**	0.594	0.615
Parietal	**1**	0.990	**1**	**1**	**0.766**	0.625
Occipital	0.984	**1**	0.938	0.979	0.547	**0.708**
Nasal	0.891	0.771	0.828	0.740	0.531	0.510
Maxilla	**1**	0.958	0.969	0.927	0.563	0.563
Lacrimal	0.953	0.927	0.984	0.958	0.734	0.542
Jugal	0.984	0.979	**1**	**1**	0.547	0.635
Total skull bone	**1**	**1**	**1**	**1**	0.578	0.531
Cranial circumference	0.984	0.948	0.984	0.875	0.531	0.635

Best AUC results in each comparison are highlighted in bold.

Table 6B

Results of univariate ROC analysis: areas under ROC curve (AUCs) are shown for (b) skull distance measurements.

(b) Skull	BA vs NC	HBA vs NC	BA vs SC	HBA vs SC	NC vs SC	HBA vs BA
Upper facial depth	0.906	0.885	0.922	0.844	0.500	0.698
Lower facial depth	0.719	0.813	0.703	0.771	0.547	0.583
Cranial circumference	0.969	0.927	0.875	0.833	0.578	0.542
Orbital height	0.547	0.542	0.844	0.781	**0.844**	0.542
Orbital width	0.734	0.698	0.781	0.792	0.578	0.646
Minimal frontal width	0.953	0.927	0.734	0.760	0.500	0.510
Bitragal width	0.891	0.865	0.906	0.844	0.531	0.656
Bigonial width	0.578	0.510	0.844	0.823	0.797	0.604
Interorbital distance	**0.984**	**0.990**	**1**	**1**	0.781	0.500
Skull Nasal length	0.625	0.750	0.625	0.677	0.547	**0.802**

Best AUC results in each comparison are highlighted in bold.

Table 6C

Results of univariate ROC analysis: areas under ROC curve (AUCs) are shown for (c) face distance measurements and cranial circumference.

(c) Face	BA vs NC	HBA vs NC	BA vs SC	HBA vs SC	NC vs SC	HBA vs BA
Nasal width	0.891	0.781	0.828	0.708	0.609	0.594
Face Nasal length	0.531	0.771	0.531	0.719	0.578	0.729
Nasal bridge length	0.531	0.802	0.500	0.719	0.516	**0.781**
Philtrum length	0.766	0.563	0.938	0.833	**0.766**	0.677
Lower facial height	0.688	0.510	0.875	0.563	0.719	0.688
Mid-facial depth	0.766	0.854	0.703	0.760	0.563	0.583
Lower facial depth	0.781	0.917	0.672	0.729	0.734	0.552
Palpebral fissure length	0.641	0.510	0.750	0.531	0.516	0.729
Inner canthal width	**1**	0.906	**0.984**	**0.906**	0.688	0.573
Outer canthal width	0.906	0.646	0.891	0.802	0.688	0.677
Cranial circumference	0.948	**0.948**	**0.984**	0.875	0.531	0.635

Best AUC results in each comparison are highlighted in bold.